Fast Synchronization Algorithms for GMSK at Low SNR in BAN

Yan Li, Yuen Sam Kwok, and Sumei Sun
Institute for Infocomm Research, A*STAR,
1 Fusionopolis Way, # 21-01 Connexis South Tower, Singapore 138632
Email: {yli, kwokys, sunsm}@i2r.a-star.edu.sg

***Abstract*—As Gaussian minimum shift keying (GMSK) modulation scheme is adopted for body area network (BAN) applications, fast and power efficient synchronization algorithms for GMSK are desired considering the limited resources in BAN. We propose new synchronization algorithms for GMSK with the constraints of low complexity and low signal-to-noise ratio. Our new feedforward timing and frequency recovery algorithms can provide much better performance than those with similar complexity in the literature. The overall bit error rate (BER) performance of the GMSK system is within 1 dB loss compared to that with perfect synchronization.**

I. Introduction

Recently, there are strong demands for body area networks (BAN) technology coming from the various parties such as medical and healthcare societies as well as information and communication industries [1]. One key challenges of BAN is the stringent power requirement, especially for the implanted medical devices. The sensors in BAN are required to have less than 1 mW power consumption, which is challenging given the wide range of data rates [1].

Gaussian minimum shift keying (GMSK) modulation scheme has been adopted in IEEE 802.15.6 for wireless BAN due to its spectral efficiency and constant-envelope property. Although GMSK has the high power and spectral efficiency, the traditional high complexity Viterbi algorithm (VA) at the receiver impedes the wide-spread usage of GMSK in BAN. We proposed a simple symbol-by-symbol (SBS) demodulator for GMSK in [2], which can achieve comparable performance to VA with a lower complexity. The proposed IQOE-demodulator in [2] is an energy-efficient, low-complexity GMSK demodulator and is suitable for BAN applications. Perfect synchronization is assumed in [2] to focus on the design of the demodulator. Here, we will extend to practical scenarios by considering imperfect synchronization caused by synchronization algorithms at the receiver.

Synchronization is a multi-parameter estimation problem. It includes the synchronization of symbol timing offset (STO), carrier frequency offset (CFO) and carrier phase offset (CPO). There are extensive research on synchronization problems. The maximum-likelihood or maximum-a-posteriori based joint estimation are of considerable theoretical interest but usually too complicated for implementation [3]. Considering the limited resources in BAN and burst transmission characteristics, fast synchronization algorithms with low complexity are necessary. Thus, we focus on feedforward synchronization methods, which can avoid the hang-up problem in feedback methods [4]. A fully digital feedforward method for joint CFO and STO estimation was proposed in [4] for MSK signals. This method cannot apply to narrow-band GMSK signals since the performance is poor [5]. Joint frequency and timing recovery method was proposed in [5] for general MSK-type modulation. The method requires to compute the combination of multiple correlation functions with different time lags, which leads to a higher complexity. In [6], joint phase and timing synchronization algorithms were proposed for MSK-type signals. However, the effects of CFO on the algorithms are not examined. Synchronization algorithms for GMSK in [7] are convenient for fully digital implementation. However, this method requires a specific training sequence pattern. Furthermore, the synchronization performance is not satisfactory for BAN applications considering the constraint of low power consumption. We will examine the synchronization for GMSK by considering all the three parameters with the constraints of low signal-to-noise ratio (SNR) and low complexity. Novel STO and CFO synchronization algorithms are proposed. Numerical simulations are used to evaluate various synchronization algorithms. Finally, the overall bit error rate (BER) performance for both uncoded GMSK systems with imperfect synchronization will be presented.

II. Overall Baseband Receiver Structure

Since coherent detection performs better than noncoherent detection, we adopt coherent detection for its power efficiency. Synchronization is necessary for coherent detection. Symbol timing synchronization is to estimate the correct sampling times to reduce the intersymbol interference. Carrier offset and phase offset caused by the unstable oscillator also need be compensated to improve the performance. In IEEE 802.15.6, preamble is used to aid the receiver in packet detection, timing synchronization and carrier-offset recovery. Each preamble is constructed by concatenating a length-63 m-sequence and a length-27 extension sequence. The entire receiver diagram is shown in Fig. 1. There are two main parts to the receiver, namely, synchronization and SBS data detection. The detection part has been discussed in [2]. We will examine the synchronization part in details in the following sections.

III. Signal Model

The complex envelope of the received baseband GMSK signal can be written as

$$r(t) = e^{j[2\pi\nu t+\theta]}s(t-\tau) + w(t) \quad (1)$$

978-1-61284-696-5/11/$26.00 ©2011 IEEE

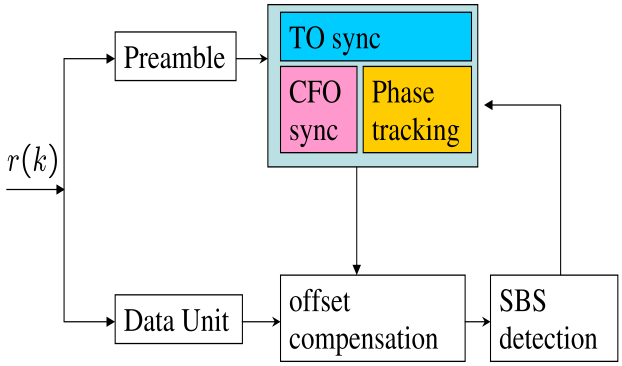

Fig. 1. Receiver Diagram with Synchronization and Detection.

where ν is the CFO, θ is the CPO, and τ is the STO. The noise process $w(t)$ is complex-valued Gaussian with independent real and imaginary components, each with two-sided power spectral density $\sigma^2 = N_0/(2E_b)$, E_b being the received signal energy per symbol. The transmitted signal $s(t)$ is given by

$$s(t) = e^{j\psi(t;\mathbf{a})} \tag{2}$$

where

$$\psi(t;\mathbf{a}) = \pi \sum_k a_k q(t-kT) \tag{3}$$

is the information bearing phase. Here, $\mathbf{a} = a_i$ are independent data symbols taking on the values of ± 1 with equal probability, T is the symbol period, and $q(t)$ is the phase pulse of the modulator, i.e., the integration of the frequency pulse $g(t)$.

To facilitate the estimation of STO, CFO and CPO, the baseband signal $s(t)$ in the nth symbol duration, i.e., $nT \le t \le (n+1)T$, is rewritten as [2]

$$e^{\psi(t;\mathbf{a})} = \exp\left(j\frac{\pi}{2}\sum_{k=0}^{n-2} a_k\right) \prod_{k=n-1}^{n} \exp\left[j\pi a_k q(t-kT)\right] . \tag{4}$$

Denote

$$\alpha_{0,n} = \exp\left(j\frac{\pi}{2}\sum_{k=0}^{n} a_k\right) \tag{5}$$

and $\alpha_{1,n} = (ja_n)\alpha_{0,n-2}$. It can be shown that $s(t)$ in (4) can be given by a linear form as [2]

$$s(t) = e^{\psi(t;\mathbf{a})} = \sum_{i=0}^{1}\sum_{k=n-2}^{n} \alpha_{i,k} h_i(t-kT) . \tag{6}$$

The possible values of $\alpha_{i,n}$ are $\{\pm 1, \ \pm j\}$. Without loss of generality, we initialize $\alpha_{0,-2} = 1$ by assuming no data being transmitted up to time $t = -T$, and $a_{-1} = 1$. Here, we decompose the nonlinear GMSK signal $s(t)$ into sums of amplitude modulated pulses in two dimensions. The pulse shaping filters are $h_0(t)$ and $h_1(t)$, respectively. In [2], we have obtained $h_0(t) = p(t-T)p(t-2T)$ for $t \in [0, 3T]$ and $h_1(t) = p(t-2T)p(t+T)$ for $t \in [0, T]$, where $p(t)$ is

$$p(t) = \begin{cases} \cos\left[\pi q(t)\right] , & t \in [0, 2T) \\ p(-t) , & t \in (-2T, 0] \\ 0 , & |t| \ge 2T . \end{cases} \tag{7}$$

For GMSK signals, the frequency pulse $g(t)$ is the convolution of a low-pass Gaussian filter with a rectangular pulse with a duration of T and a magnitude of $1/(2T)$, i.e.,

$$g(t) = \frac{1}{2T}\left\{Q\left[\frac{2\pi B}{\sqrt{\ln 2}}\left(t - \frac{3T}{2}\right)\right] - Q\left[\frac{2\pi B}{\sqrt{\ln 2}}\left(t - \frac{T}{2}\right)\right]\right\} . \tag{8}$$

Here, B is the 3-dB bandwidth of the Gaussian low-pass filter, and $Q(x) = 1/\sqrt{2\pi}\int_x^\infty e^{-t^2/2}dt$. The frequency pulse $g(t)$ is usually time truncated to the interval $[0, LT]$ and is normalized, i.e., $\int_0^{LT} g(t)dt = \frac{1}{2}$. In IEEE 802.15.6, the design parameter BT is 0.5. For $BT = 0.5$, we can choose $L = 2$ since $g(t)$ is almost zero for $t > 2T$.

Replacing $s(t)$ using its linear expression in (6), we can rewrite the signal model (1) in a discrete form as

$$\begin{aligned} r_{k,n} &= e^{j\left[2\pi\nu(kT + n\frac{T}{N}) + \theta\right]} \times \\ &\quad \sum_{i=0}^{1}\sum_{l=k-2}^{k} \alpha_{i,l} h_k\left((k-l)T + n\frac{T}{N} - \tau\right) + w_{n,i} \end{aligned} \tag{9}$$

Here, $r_{k,n}$ and $w_{n,i}$ denote the samplers of the received signal and the noise at time $t = kT + n\frac{T}{N}$, respectively, where N is the oversampling rate. $T_s = \frac{T}{N}$ is the sampling time. This linear representation form of GMSK is similar to that of PAM modulation but with inter-symbol interference (ISI). For the extreme case of no ISI, the signal can be reduced to MSK. Thus, this motivates us to propose new synchronization methods for GMSK by combining those methods for MSK and the methods of reducing noise/interference.

IV. Symbol Timing Offset Estimation

As mentioned, the MCM method proposed in [4] is specifically designed for MSK, and its performance with GMSK is found to be poor. However, the feedforward structure of this timing recovery method is quite efficient for burst transmission. We will modify this known method and apply it to GMSK. It turns out that significant improvements can be achieved by our modified TO estimation algorithm.

The key idea in the MCM method is to use the nonlinear combinations of delayed versions of the baseband signal which contain periodic components that can be exploited for clock recovery. The following fourth-order nonlinear transform is commonly used in synchronization for MSK-type signals:

$$z(t) = \mathrm{E}\left\{\left[x(t)x^*(t-mT)\right]^2\right\} \tag{10}$$

where $\mathrm{E}\{\cdot\}$ denotes expectation operation, and m is an integer. It has been shown in [5] that if $x(t) = r(t)$, $z(t)$ is given by

$$z(t) = e^{j4\pi m\nu T} g(t-\tau) + n(t) \tag{11}$$

where $n(t)$ is a noise term and the periodic signal $g(t)$ is

$$\begin{aligned} g(t) &= \mathrm{E}\left\{e^{j2[\psi(t;\mathbf{a}) - \psi(t-mT;\mathbf{a})]}\right\} \\ &= \prod_{k=-\infty}^{\infty} \cos\left(2\pi\left[q(t-kT) - q(t-(k+m)T)\right]\right) . \end{aligned} \tag{12}$$

Thus, the timing information can be extracted from $z(t)$. In the MCM method [4], $m = 1$ is used for MSK signals. To improve the performance for GMSK, several periodic signals with different values of m are combined together to estimate TO in [5]. The drawback of this method is the increased complexity. Here, we simply use one correlation function with $m = 2$. The structure is similar to the MCM method which can be easily implemented in hardware. However, the received signal $r(t)$ is first filtered by using a low-pass filter to improve the SNR for TO estimation. The matched filter is used to maximize the SNR at the receiver. From (6), a bank of two matched filters is optimum to maximize the SNR of the received GMSK signal. However, considering $h_1(t) << h_0(t)$ [2], we will just use one-dimensional matched filter $h_0(t)$ at the receiver to reduce complexity. Then, the output of the matched filter is fed into TO estimator. Thus, the key difference of our method and those in [4] and [5] is the input to the nonlinear transform function. In our method, the $x(t)$ is

$$x(t) = r(t) \otimes h_0(-t) \tag{13}$$

Denote $x_{k,n} = x(t)|_{t=kT+nT_s}$. The full digital timing synchronization is given by

$$\hat{\tau} = -\frac{T}{2\pi} \arg \sum_{n=0}^{N-1} \left\{ \sum_{k=0}^{L_T-1} [x_{k,n} x^*_{k-2,n}]^2 \right\} e^{-j2\pi n/N} \tag{14}$$

where $\arg(\cdot)$ denotes the phase operation, and L_T is the observation duration for timing synchronization. The simulation results show that there is much improved performance of our method compared to the MCM method, especially at low SNR.

V. Carrier Frequency Offset Estimation

With the estimated STO, the received signals are interpolated to obtained the samplers at the correct sampling time. Then, the time synchronized received signals are used for CFO estimation. With the preamble, data-aided CFO estimate methods can be used. Fitz estimator proposed in [9] is one of the widely used frequency estimator due to its accuracy and easy implementation. The method uses the phase of the correlation of the delayed versions of the demodulated signals. However, the accuracy of this estimator is dependent on the value of the delay. To achieve better estimation accuracy, a large value of the delay is required, which leads to a smaller synchronization range. In BAN applications, there may require a wider synchronization range due to the hardware limitation. Then, the delay cannot be too large. The maximum delay is upper bounded by

$$D_{max} < \frac{1}{2|\nu_{max}|T} \,. \tag{15}$$

Due to the limitation of the maximum delay, the accuracy of CFO estimation using the traditional Fitz method at the symbol level may not be satisfied. We thus extend the Fitz method to the sample level as following. The sampling of the demodulated signal is denoted as

$$\begin{aligned} y(iT_s) &= r(iT_s)s^*(iT_s - \hat{\tau}) \\ &= e^{j[2\pi\nu(kT+nT_s)+\theta+\phi(iT_s)]} + n'(iT_s) \end{aligned} \tag{16}$$

where $k = \lfloor \frac{i}{N} \rfloor$, and $n = i - Nk$. The phase $\phi(iT_s)$ is caused by timing estimation error, and $n'(iT_s)$ is a zero-mean noise term. When timing estimation is accurate, we can neglect the effects of $\phi(iT_s)$. The estimation of ν is given by

$$\hat{\nu} = \frac{1}{\pi D(ND+1)T} \sum_{m=1}^{ND} \arg R(m) \tag{17}$$

where D is a parameter less than D_{max}, and $R(m)$ is

$$R(m) = \frac{1}{NL_f - m} \sum_{i=m}^{NL_f-1} y(iT_s)y^*((i-m)T_s) \,. \tag{18}$$

L_f is the observation duration for CFO estimation. Comparing with eq. (30) in [9], our method is operating at sample level which can significantly improve the estimation performance. This is because the delay length at the sample level is effectively increased by multiples of the oversampling rate N.

VI. Carrier Phase Offset Estimation

The CFO caused phase rotation in $y(iT_s)$ can be compensated by using the estimated $\hat{\nu}$ in (17). After CFO compensation, the CPO estimation can be directly obtained as

$$\hat{\theta} = \tan^{-1} \frac{\sum_{i=0}^{L_\theta-1} \Im[y_c(iT_s)]}{\sum_{i=0}^{L_\theta-1} \Re[y_c(iT_s)]} \tag{19}$$

where $\Re[\cdot]$ and $\Im[\cdot]$ denote the real and imaginary part of a complex, respectively. L_θ is the observation duration for phase synchronization, and $y_c(iT_s)$ is the CFO-compensated demodulated signal given by

$$y(iT_s) = e^{-j[2\pi(kT+nT_s)\hat{\nu}]} y(iT_s) \tag{20}$$

where $k = \lfloor \frac{i}{N} \rfloor$ and $n = i - Nk$. It is worth noting that the value of L_θ is based on the varying property of the phase. In general, the larger value of L_θ brings a better phase estimation, provided that the phase θ is constant over the duration of L_θ. However, due to the residue CFO caused by imperfect frequency estimation, the phase is slowly changing over time. Thus, the value of L_θ cannot be larger than the coherence time of the phase process. With the aid of preamble, an initial estimate of the phase θ can be obtained. This phase estimate will be updated during the data transmission using the same method with data-decision feedback.

VII. Numerical Results

The frequency band for GMSK modulation defined in IEEE 802.15.6 is 420-450 MHz. The supported data rate is 151.8 kbps. Assuming the local oscillator has $\pm$20ppm variation for carrier frequency, the maximum CFO will be $\nu_{max} = 18$ kHz, and the maximum normalized CFO will be within the range of $[-0.1,\ 0.1]$. The STO and PO are assumed to be uniformly distributed among $[-0.5T,\ 0.5T]$ and $[-\pi,\ \pi]$, respectively. In simulations, random values for CFO, STO, and PO are used for each implementation. Given the preamble structure, the observation durations L_T, L_f and L_θ are 90, 63 and 27, respectively.

Fig. 2 and Fig. 3 show the performance comparison between our proposed method and those in the literature for TO and

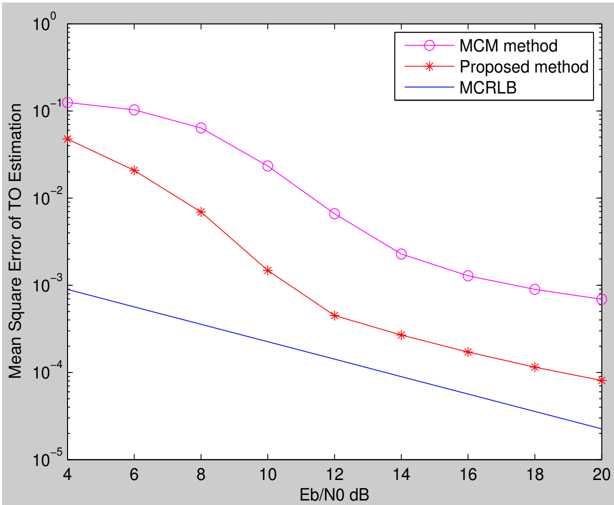

Fig. 2. Performance comparison of different timing synchronization for GMSK.

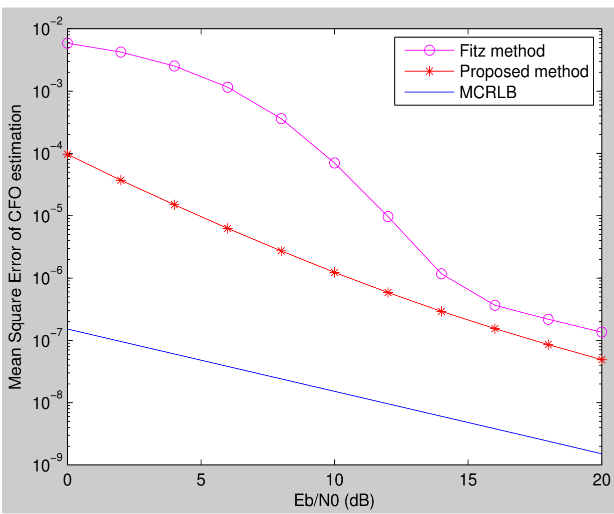

Fig. 3. Performance comparison of different CFO synchronization for GMSK.

CFO estimation, respectively. The estimation performance is evaluated using the mean square error. The modified Cramer-Rao bound (MCRB) in [10] is used as a benchmark. For CFO estimation, $D = 2$ is chosen due to the maximum value of the normalized CFO. The results show that our methods can provide much improved TO and CFO estimation, especially for low SNR. Our proposed methods can achieve similar performance to those in [5] but with reduced complexity.

In Fig. 4, the overall BER performance of GMSK over AWGN channel with our synchronization algorithms is presented. Differential-encoded IQOE demodulator in [2] is used for SBS data detection. Compared to the perfect synchronization case, the overall performance loss caused by imperfect TO, CFO and PO estimation is less than 1 dB.

VIII. Conclusions

Improved feedforward timing and frequency synchronization algorithms were proposed. The feedforward structure

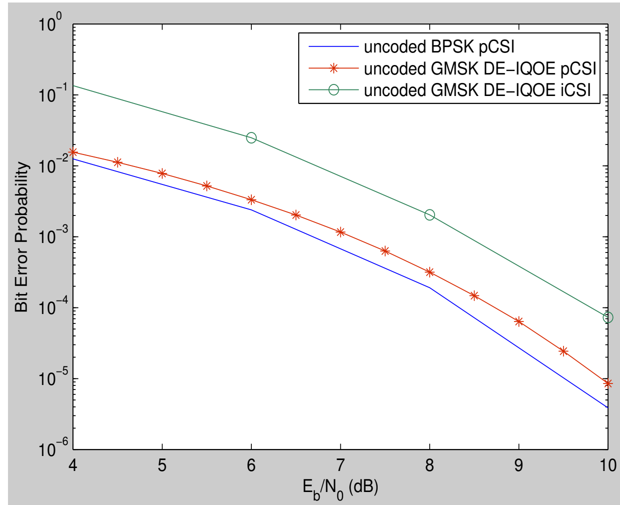

Fig. 4. BER performances of GMSK over AWGN with perfect and imperfect synchronization.

adopted can be easily implemented in hardware and can avoid hang-up problem. These advantages are suitable for burst transmission mode in BAN. Due to the low SNR operation constraints in BAN, we propose the use of the matched filter to maximize SNR at the receiver which then leads to improved timing synchronization performance. For CFO estimation, a sample-level method is proposed to handle the wide synchronization range caused by hardware limitation.

References

[1] H-B Li and R. Kohno, "Introduction of SG-BAN in IEEE 802.15 with related discussion," *in Proc. ICUWB*, pp. 134-139, Sept. 2007.

[2] Y. Li, Y. Kwok and S. Sun, "Energy Efficient Low-Complexity Symbol-by-Symbol GMSK Demodulator for BAN," *accepted by IEEE VTC 2011 Spring*, May, 2011.

[3] R. W. D. Booth, "An illustration of the MAP estimation method for deriving closed-loop phase tracking topologies: The MSK signal structure," *IEEE Trans. Commun.*, vol. COM-28, pp. 1137-1142, Aug. 1980.

[4] R. Mehlan, Y. Chen, and H. Meyr, "A fully digital feedforward MSK demodulator with joint frequency offset and symbol timing estimation for burst mode mobile radio," *IEEE Trans. Vehicular Tech.*, vol. 42, pp. 434-443, Nov. 1993.

[5] M. Morelli and U. Mengali, "Joint frequency and timing recovery for MSK-type modulation," *IEEE Trans. Commun.*, vol. 47, pp. 938-947, Jun. 1999.

[6] M. Morelli and G. M. Vitetta, "Joint phase and timing synchronization algorithms for MSK-type signals," *IEEE Communication Theory Mini-Conference*, pp. 146-150, Jun. 1999.

[7] Y-L Huang, K-D Fan and C-C Huang, "A fully digital noncoherent and coherent GMSK receiver architecture with joint symbol timing error and frequency offset estimation," *IEEE Trans. Vehicular Techno.*, vol. 49, pp. 863-874, May. 2000.

[8] P. Laurent, "Exact and approximate construction of digital phase modulations by superposition of amplitude modulated pulses (AMP)," *IEEE Trans. Commun.*, vol. COM-34, pp. 150-160, Feb. 1986.

[9] M. P. Fitz, "Planer filtered techniques for burst mode carrier synchronization," *in Proc. Globecom*, vol. COM-43, pp. 1169-1178, 1991.

[10] U. Mengali and A. N. D'Andrea, *Synchronization techniques for digital receiver*, Plenum Press, New York, 1997.